SoftwareX 20 (2022) 101242

Contents lists available at ScienceDirect

SoftwareX

journal homepage: www.elsevier.com/locate/softx

Original software publication

XTBDFT: Automated workflow for conformer searching of minima and transition states powered by extended tight binding and density functional theory

Sibo Lin [a,*], Mohamed Elanany [b], Motaz Khawaji [b]

[a] Aramco Services Company: Aramco Research Center – Boston, 400 Technology Sq., Cambridge, MA, 02139, USA
[b] Saudi Aramco Research Center at KAUST, Thuwal, Saudi Arabia

ARTICLE INFO

Article history:
Received 7 June 2022
Received in revised form 3 October 2022
Accepted 18 October 2022

Keywords:
Density functional theory
Extended tight binding theory
Automated workflow
Molecular modeling
Conformer
Transition state
Organometallic
Metal complex

ABSTRACT

Recent developments have greatly increased accuracy, applicability, and accessibility of extended tight binding theory (XTB), allowing for rapid semi-empirical quantum mechanical calculations of molecular potential energy surfaces. For finer thermochemical accuracy, density functional theory (DFT) calculations are still required on stationary points. Such multi-level simulations present a steep learning curve, and trained researchers must spend significant time monitoring calculations and managing the workflow. Herein, we present XTBDFT, the first automated workflow between all freely licensed engines for XTB, DFT, and helper modules. In this version, the specific engines are GFN-XTB/CREST, NWChem, and GoodVibes, respectively. Example applications of this workflow is presented, finding the lowest energy conformer of a metal complex with multiple hindered degrees of internal rotation.

Code metadata

Current code version	*V1.0.0*
Permanent link to code/repository used of this code version	https://github.com/sibo/xtbdft/releases/tag/v1.0.0
Code Ocean compute capsule	*none*
Legal Code License	*MIT*
Code versioning system used	*git*
Software code languages, tools, and services used	*Python 3.x*
Compilation requirements, operating environments & dependencies	*Unix/Linux computing cluster with workload management package (at present Moab/Torque or Slurm), XTB engine (at present CREST and GFN2-xTB), DFT engine (at present NWChem), and quasi-harmonic frequency correction engine (GoodVibes)*
If available Link to developer documentation/manual	*none*
Support email for questions	sibo.lin@aramcoamericas.com

1. Motivation and significance

Computational optimization of a molecule to its global minimum-energy structure is a complex challenge, but necessary for accurate computational prediction of thermodynamics and energy barriers [1,2]. Density functional theory (DFT) softwares implement geometry optimization algorithms that locate nearby local minima [3]. Researcher-directed generation and exploration of every local minimum (“conformer”) is resource-intensive and error-prone for large and complex molecules, and such researcher-directed approaches cannot be incorporated into the ultimate goal of autonomous molecular design [4]. Automated conformer searching remains a “holy grail” research target in the field of computational chemistry [5]. Classical force field (FF) driven conformational searches, as implemented in many existing codes, are computationally efficient and can be scaled to address folding conformations of macromolecules such as proteins [6,7]. However, FF are typically parameterized against a select group of elements and functional groups, and may perform poorly for exotic molecules, such as those containing heavy atoms, unusual

* Corresponding author.
E-mail address: sibo.lin@aramcoamericas.com (Sibo Lin).

https://doi.org/10.1016/j.softx.2022.101242

functional groups, or transition metal centers, or for saddle-point transition states [8–10].

GFN2-xTB, an open-source, semi-empirical extended tight binding theory implementation recently developed by Prof. Stefan Grimme, offers a path forward. GFN2-xTB proceeds orders of magnitude faster than DFT, yet achieves similar geometric accuracy across a wide range of molecules and atoms (H through Rn) [11]. Grimme's open-source Conformer-Rotamer Ensemble Sorting Tool (CREST) iteratively employs GFN2-xTB, meta-dynamic sampling, and genetic z-matrix crossing steps to efficiently generate a diverse conformer ensemble and preliminarily rank their energies [1,12]. Further automated refinement of these conformers with commercial (closed-source) DFT programs Orca or Turbomole has been implemented in ENSO and CENSO [13,14]. Semi-automated conformational modeling has also been implemented with Gaussian as the closed-source DFT engine [15].

Herein, GFN2-xTB and CREST have been interfaced with NWChem [16] for an automated, multi-level workflow called XTBDFT to find and evaluate lowest energy conformations of minima and saddle points. Unlike previous implementations relying on more restrictively licensed DFT engines, XTBDFT uses NWChem (Educational Community License) and an end-to-end open-source computational workflow. This choice allows for freely licensed, efficient, widely distributed, and readily customizable operation on any Linux/Unix computing cluster. Additionally, XTBDFT's operational code is contained in one file and requires minimal Python library dependencies, which facilitates installation on air-gapped computing clusters.

We applied an earlier version of this software in our study of diphosphinoamine ligands for ethylene tetramerization catalysis [17]. Diphosphinoamines and their iminobisphosphine isomers have numerous hindered degrees of internal rotation, and manual generation of the conformers would be a tedious process. Using conventional molecular mechanics or semiempirical conformational searches could result in inaccurate geometries and initial energy rankings, as those techniques may be poorly parameterized for unusual functional groups (e.g. diphosphinoamine and iminobisphosphines). This software has been used to screen novel diphosphinoamine ligand candidates from our research group and from our collaborators at King Fahd University of Petroleum and Minerals (KFUPM), leading to discovery of breakthrough catalysts for ethylene tetramerization [17,18]. In this report, we describe the technical operation of XTBDFT along with new features derived from applying bond constraints: organometallic conformer searching, transition state location, and transition state conformer searching.

2. Software description

Environment pre-requisites for XTBDFT are a Unix computing cluster with a workload management system (at present Moab/Torque or Slurm), GFN2-xTB, CREST, NWChem, and GoodVibes. GFN2-xTB and CREST binaries, code, and documentation are available at https://github.com/grimme-lab/xtb and https://github.com/grimme-lab/crest, respectively. Pre-compiled binaries of NWChem can be installed via common Unix repositories with the *apt* (Debian) or *rpm* (Red Hat) commands; however, for optimal performance, NWChem source code from https://github.com/nwchemgit/nwchem should be compiled. For convenience, a shell script that sets up all the pre-requisite softwares (with the exception of the workload management system) has been included with XTBDFT (`complete_install.sh`).

XTBDFT currently has two types of workflows, *autoConf* and *autoTS*, as illustrated in Fig. 1. In *autoConf* mode, there are four phases for finding and evaluating the minimum energy conformation: (1) Running CREST to generate an ensemble of low-energy conformers from an input .xyz file, (2) refining the conformers with lower-level NWChem DFT optimization, (3) running a high-level NWChem DFT optimization on the minimum-energy conformation, and (4) determining quasi-harmonic frequency calculations using GoodVibes [19]. In *autoTS* mode, there are five phases, the last four of which are similar to *autoConf* mode: (0) The input .xyz file for the reactant is first scanned along a specified reaction coordinate to find a product geometry, and GFN-xTB meta-dynamics path finding is applied to find a reasonable transition state geometry [20]. Then (1) CREST conformer search and (2) NWChem ensemble refinement are performed while constraining the reaction coordinate at a fixed value near the transition state. (3) The lowest energy conformation is then optimized to the nearest saddle point (transition state) without geometrical constraints, and (4) quasi-harmonic frequency corrections are applied. For reaction coordinate specification, only a single interatomic distance coordinate is currently supported. XTBDFT may not perform well for multi-centered reactions that cannot be well-defined by a single interatomic distance (e.g. Diels–Alder concerted cycloaddition, internal rotation of a dihedral angle, outer-sphere hydride transfer). However, XTBDFT's *autoTS* mode is utilized regularly in our industrial setting to study elementary organometallic reactions: oxidative addition, reductive elimination, migratory insertion/elimination.

XTBDFT launches this workflow and automates data exchange between the various phases. The guess geometry in .xyz file format and several optional parameters are specified via command line arguments:

`xtbdft.py guess.xyz [-chrg` *`int`*`] [-uhf` *`int`*`] [-xc` *`xc1,xc2,xc3,xc4`*`] [-bs` *`bs1,bs2,bs3,bs4`*`] [-mode autoConf|autoTS` *`atom1_index atom2_index finalScanDistance_Ang`*`] [-other=[''skipCrest''|`*`crestParameters`*`]`

The square brackets denote optional parameters that do not have to be specified for a calculation to proceed (but may be necessary to accurately describe the chemical system of interest, for instance if it is cationic or has unpaired electrons). If the only input parameter is the initial geometry .xyz file, then the other parameters will default to the values listed in Table 1, which are the parameters utilized in our recent study on diphosphinoamine ligand stability. Functionals and basis sets are defined with strings, as described in the NWChem documentation, and listed in a comma-delimited command-line argument of the format xc1,xc2,xc3,xc4 or bs1,bs2,bs3,bs4 (no spaces are permitted in the comma-delimited list). The initial DFT ensemble geometry optimization is performed with xc1/bs1. The geometry-optimized ensemble can be further evaluated with single-point energy calculations at the xc2/bs2 level of theory to determine the lowest energy conformation. Alternatively, the lowest-energy conformation can be determined directly from xc1/bs1 geometry optimization energies, saving computational time, by entering no characters for xc2 and bs2, as is the case for the default procedure listed in Table 1. The lowest energy conformation is then further geometry optimized to tighter criteria at the xc3/bs3 level of theory, and finally a single-point energy is calculated using xc4/bs4. For all DFT calculations, Grimme's DFT-D3 semiempirical dispersion correction is applied [21,22].

In a previous application of XTBDFT for main group compounds, the conformer ensemble refinement phase utilized the NWChem *medium* integration grid and the smaller def2-SV(P) basis set as bs1 during conformer ensemble refinement phase [17]. However, finer integration grids have been shown to be critical for accurately evaluating organometallic reaction energies and barriers [23,24]. Additionally, the slightly larger Weigend-Ahlrichs def2-SVP basis set [25,26], which includes polarization functions for hydrogen atoms, has commonly been used for geometry optimization in organometallic theoretical studies [27].

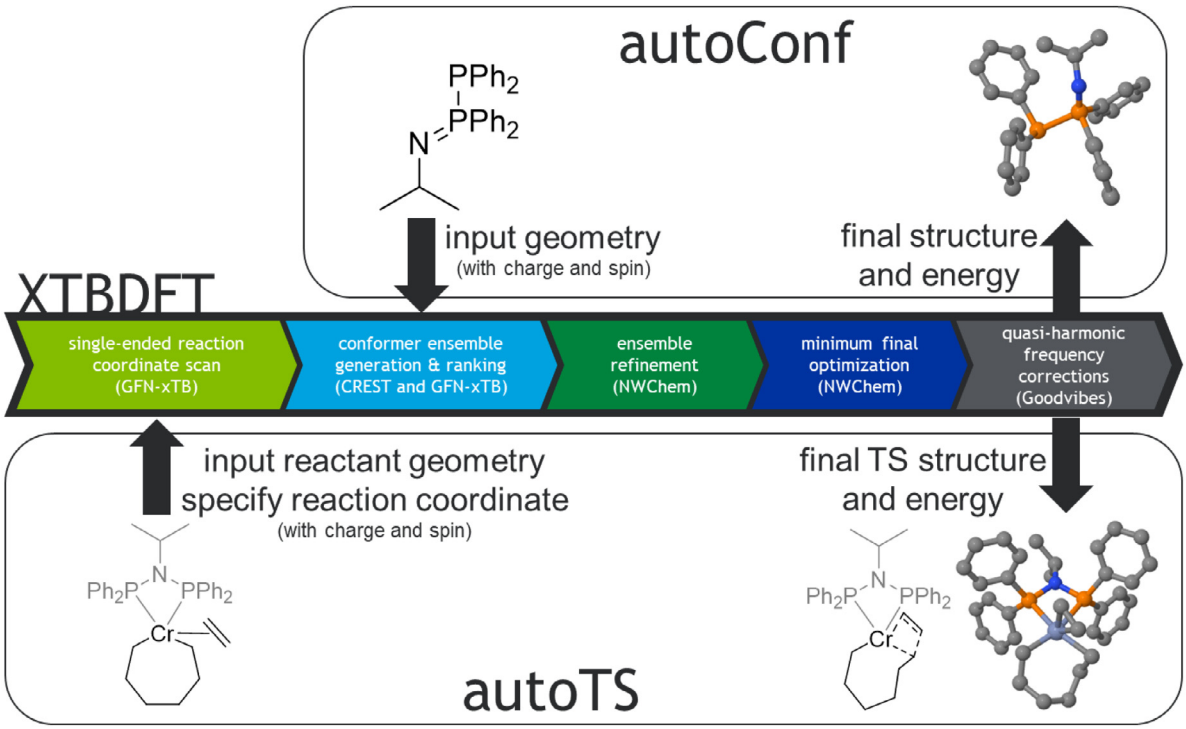

Fig. 1. XTBDFT workflows in autoConf and autoTS modes.

Table 1
Optional command-line parameters.

Flag	Parameter	Default
`-chrg`	Charge of species	`0`
`-uhf`	Unpaired electrons	`0`
`-xc`	Comma-delimited list of xc1-xc4 (no spaces)	"`b3lyp,,b3lyp,b3lyp`"
`-bs`	Comma-delimited list of bs1-bs4 (no spaces)	"`def2-svp,,def2-svp,def2-tzvp`"
`-cutoff`	kcal/mol cutoff of conformers to optimize with xc1/bs1	`3.0`
`-mode`	"autoConf" -or- "autoTS *atom1_index atom2_index finalScanDistance_Ang*"	"`autoConf`"
`-other`	"skipCrest" -or- any valid CREST command-line parameters, e.g. *-other="-cbonds 1.0"* or *-other="-cmetal 0.2"*	`None`

Thus in order to better treat organometallic compounds, XTBDFT's default integration grid and basis set bs1 during conformer refinement have been upgraded to NWChem's *fine* setting and def2-SVP.

In some instances, the default meta-dynamics conformer search pushes too far away from the provided guess geometry in an *autoConf* or *autoTS* calculation. For instance, PhCl is a common solvent for early transition metal catalysis [28]. PhCl solvent molecules may also act as ligands to the metal center, either through a dative bond from a Cl lone pair [29,30] or through an η^6-arene interaction [29–32]. In attempting to explore the conformational space of bis(η^6-chlorobenzene)chromium cation, however, the default meta-dynamics parameters of CREST artificially favor oxidative addition of the C–Cl bond despite the experimental isolability of the sandwich complex. To prevent C–Cl oxidative addition, either the CREST phase can be skipped, and only the input guess conformer is evaluated (`-other=''skipCrest''`); or any valid CREST command-line parameters may be used to modify the meta-dynamics search. To resist C–Cl cleavage of PhCl ligands, for example, the cbonds flag can be utilized to constrain the input bond lengths with an added harmonic potential (`-other=''-cbonds 0.002''`). Refer to the CREST documentation for other CREST command-line parameters. With the cbonds option, six distinct conformers were found by XTBDFT (Fig. 2, **A**–**F**). Note similar conformers **D** and **E**, which likely would not be considered separately in a human-directed conformer search, yet retain an energy difference of 0.49 kcal/mol after DFT geometry optimization at the B3LYP+D3/def2-TZVP level of theory. The lowest energy *trans* conformation **C** matches that observed via crystallography for the related bis(η^6-toluene)chromium cation [33]. The cbonds flag is not applied by default in XTBDFT, as searching for the minimum energy conformation of metal complexes with hemilabile ligands requires making and breaking metal-ligand bonds.

Currently, applying effective core potentials or different basis sets to specific atoms (e.g. def2-TZVP for transition metal center and def2-SVP for all other atoms) is not supported, but will be implemented in a future version of XTBDFT. Other features to be implemented include allowing other input file formats (.mol, .pdb, .cif, etc.) and automating thermochemistry tabulation from GFN2-xTB and NWChem output text files. To facilitate future development and code versioning, XTBDFT will be hosted at https://github.com/sibo/xtbdft

3. Illustrative examples

Example 1 (*Automated Conformer Search (autoConf mode)*)**.** XTBDFT was used to evaluate the thermodynamic stability of PNP ligand N-isopropyl-bis(diphenylphosphino)amine against its PPN isomer, N-isopropyl-P,P,P',P'-tetraphenyl-iminobisphosphine. This

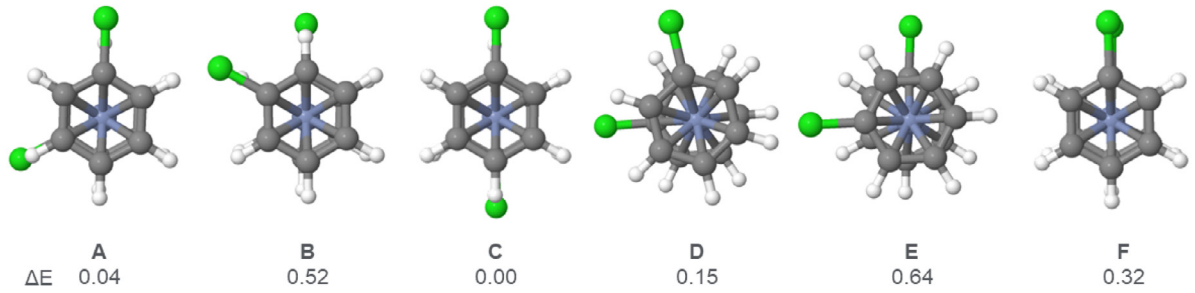

Fig. 2. XTBDFT Conformer search of $[Cr(\eta^6\text{-}C_6H_5Cl)_2]^+$ (doublet spin) with -other="-cbonds 0.02" option. Relative energies (kcal/mol) shown are after DFT re-optimization at the B3LYP+D3/def2-TZVP level of theory.

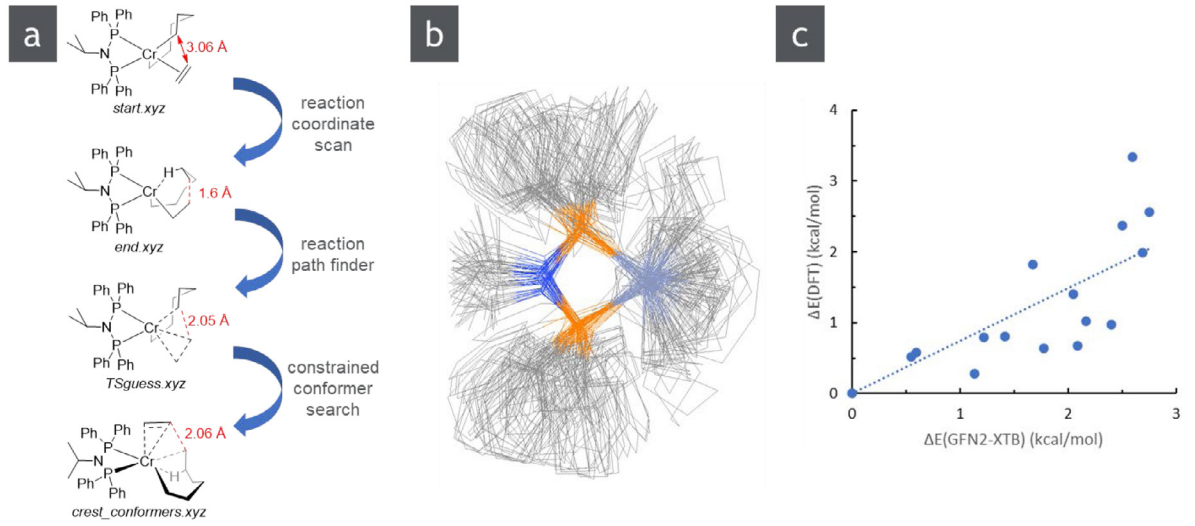

Fig. 3. XTBDFT autoTS results: (a) structures generated with GFN2-xTB and CREST (only the first frame of *crest_conformers.xyz* is shown); (b) overlaid image of 69 structures of *crest_conformers.xyz* with ΔE(GFN2-xTB) < 6.0 kcal/mol; (c) ΔE(DFT) after DFT re-optimization vs ΔE(GFN2-xTB) of lowest-energy conformations of *crest_conformers.xyz*. All structures have +1 charge and quartet spin state.

isomerization energy may be related to the relative propensity of different PNP ligands to form undesired polyethylene byproduct during ethylene tetramerization catalysis [17,34]. A starting geometry file (*guess.xyz*) for each molecule was generated with molview [35], and then the lowest energy conformation was determined by entering:

```
xtbdft.py guess.xyz > autoConf.out
```

XTBDFT analyzes 35 unique conformers of the PNP ligand in a 6 kcal/mol window at the CREST/GFN2-xTB level of theory. The PPN isomer (illustrated in Fig. 1) has 62 unique conformers at the same level of theory. Manually generating such large ensembles would be inefficient and inconsistent, and conventional molecular-mechanics driven conformational searches would not yield as accurate geometries or relative energies due to the unusual P-P=N or P-N-P moiety. In the XTBDFT autoConf workflow, this conformer ensemble is then refined with NWChem to yield the lowest energy conformer with no further human intervention. As an added benefit of using CREST for conformational searching, it groups rotamers that are nearly equivalent (for instance, related by ∼180° rotation of a phenyl substituent), greatly reducing the size of the conformer ensemble before optimization with higher levels of theory. For comparison, the Merck Molecular Force Field [36] (MMFF) conformer search built into Spartan '20 gives 144 conformers of N-isopropylbis(diphenylphosphino)amine in a 6 kcal/mol window.

Example 2 (*Automated Transition State Search (autoTS mode)*)**.** XTBDFT was used to find and evaluate an ethylene insertion transition state structure, critical to computational design of ethylene oligomerization catalysts. First, a reasonable reactant geometry (`start.xyz`, Fig. 3a) was quickly generated with a combination of molview and GFN2-xTB geometry optimization. Visual examination of `start.xyz` revealed that carbon atoms C28 and C65 were 3.06 Å apart but aligned to form a C–C bond (which are typically ∼1.54 Å). Thus, the reaction coordinate was defined as shrinking the distance between atoms 26 and 80 to 1.6 Å. In order to prevent unintended skeletal isomerization, all bonds were also constrained with a harmonic potential with force constant of 1.0 Hartree/Bohr^2:

```
xtbdft.py start.xyz -chrg 1 -uhf 3 -mode autoTS 28 65
1.6 -other="-cbonds 1.0" > autoTS.out
```

Without any further researcher intervention, several calculations are performed. In GFN2-xTB and CREST these steps are illustrated in Fig. 3a: (1) the product of the reaction coordinate scan is determined (`end.xyz`); (2) a meta-dynamics reaction path finder is used to find the transition state guess (`TSguess.xyz`); and (3) the reaction coordinate is held fixed as metadynamics conformer search is performed to return a conformer ensemble (`crest_conformers.xyz`). Then with DFT: (4) the reaction coordinate is again held fixed as the conformer ensemble is geometry optimized; (5) the lowest energy conformer is then optimized to a saddle point with no geometric constraints; and (6)

vibrational and single-point energy corrections for the final geometry are determined to allow for high-level thermochemistry calculations.

Note that in this example, 69 unique conformations of the ethylene insertion transition state were found with ΔE(GFN2-xTB) < 6.0 kcal/mol (Fig. 3b), which is much too many for a human researcher to efficiently generate via manual intuition. Upon initial DFT geometry re-optimization of the lowest-energy conformers, there was good correlation between ΔE(DFT) and ΔE(GFN2-xTB) (Fig. 3c, $R^2 = 0.85$), demonstrating the utility of GFN2-xTB calculations to quickly generate organometallic transition state conformer ensembles for further refinement with DFT calculations.

4. Impact

This is the main section of the article and the reviewers weight the description here appropriately

This is the first example that implements an automated workflow for composite xTB-DFT conformational searches using all open-source software. The no-cost, relaxed licensing terms of the underlying computational chemistry codes (currently GFN2-xTB, CREST, NWChem, and GoodVibes) allows for broad adoption across the chemistry and machine-learning communities, along with wide-scale distribution across large computing clusters and on-demand cloud computing instances. The lightweight codebase of XTBDFT facilitates adoption, modification, and contribution by other researchers. This allows computational chemists to find lowest energy conformers of systems without stumbling over the intricacies of setting up specialist input files for different programs. Even for trained computational chemists, the automated workflow will save significant researcher time that is usually spent monitoring calculations and transferring data from one program to another.

It has been common practice for DFT computational chemists to select one or a handful of input geometries for geometry optimization. However, such processes are fallible and time-intensive for all but the simplest molecules. An alternative has been using molecular dynamics (powered by molecular mechanics) to survey a variety of starting geometries for DFT optimization. The underlying molecular mechanics is often not parameterized for molecules containing transition metals or unusual chemical functional groups. XTBDFT allows for optimization to a global minimum for molecules containing elements H-Rn.

XTBDFT facilitates study of computationally challenging organometallic catalysts. We are applying XTBDFT to study the mechanism of Cr-PNP catalysts for ethylene oligomerization. Previous DFT studies using simplified bidentate ligands have shared few details on how the conformer spaces of these intermediates and transition states were searched [27,37–40]. In one study on related Cr-dipicolylamine metallocycle intermediates [41], in order to utilize the Tinker MMFF [42] conformational search, the authors computationally transmuted Cr to Si, which (a) artificially disfavors four-coordinate square planar complexes and (b) does not allow accurate conformational searching of transition states or higher-coordinate species (e.g. ethylene adducts preceding chain growth). XTBDFT is able to directly treat organometallic species with greater accuracy than FF methods.

Finding transition states is critical for catalyst design, as the energy barriers for reaction pathways will determine catalyst activity and selectivity. Yet locating initial transition state guess structures remains a challenging process that is often reliant on human intuition. Many transition-state localization procedures [9,43,44], including the one built into GFN2-xTB, are "double-ended", requiring input of reactant and product geometries with painstakingly identically ordered atoms [20]. Additionally, higher-level DFT calculations are still required to determine accurate thermochemistry for transition state geometries located by GFN2-xTB. XTBDFT has the capability to (a) implement a "single-ended" transition state search [45], in which only the reactant geometry and a reaction coordinate needs to be provided, and (b) automate the workflow between GFN2-xTB and NWChem, two specialist programs that are not natively able to transfer data to each other.

5. Conclusions

XTBDFT performs conformational searches by automating the workflow from all open-source chemistry programs: GFN2-xTB/CREST, NWChem, and Goodvibes. It also simplifies the calculation setup in that the user does not need to know specific input file formats for the various programs; instead, all of the key parameters can be specified directly on the command line. Unlike other conformational searches driven by molecular mechanics, XTBDFT is driven by semi-empirical quantum mechanics that is parameterized for elements H–Rn and potentially applicable to transition state optimization. XTBDFT has been applied in our research group to study ligands for ethylene tetramerization catalysis, and we expect it to find a variety of applications for conformationally flexible molecules.

Declaration of competing interest

The authors declare that they have no known competing financial interests or personal relationships that could have appeared to influence the work reported in this paper.

Data availability

In Code metadata table, a permanent link to the github repository of this code version is listed.

Acknowledgments

S.L. is grateful to Stefan Grimme for assistance with setting up GFN2-xTB and CREST; to Sivakumar Nanjundan for Aramco Americas computing cluster maintenance.

References

[1] Pracht P, Bohle F, Grimme S. Automated exploration of the low-energy chemical space with fast quantum chemical methods. Phys Chem Chem Phys 2020;22:7169–92. http://dx.doi.org/10.1039/C9CP06869D.
[2] Ryu H, Park J, Kim HK, Park JY, Kim S-T, Baik M-H. Pitfalls in computational modeling of chemical reactions and how to avoid them. Organometallics 2018;37:3228–39. http://dx.doi.org/10.1021/acs.organomet.8b00456.
[3] Li X, Frisch MJ. Energy-represented direct inversion in the iterative subspace within a hybrid geometry optimization method. J Chem Theory Comput 2006;2:835–9. http://dx.doi.org/10.1021/ct050275a.
[4] dos Passos Gomes G, Pollice R, Aspuru-Guzik A. Navigating through the Maze of homogeneous catalyst design with machine learning. Trends Chem 2021;3:96–110. http://dx.doi.org/10.1016/j.trechm.2020.12.006.
[5] Houk KN, Liu F. Holy grails for computational organic chemistry and biochemistry. Acc Chem Res 2017;50:539–43. http://dx.doi.org/10.1021/acs.accounts.6b00532.
[6] Dill KA, MacCallum JL. The protein-folding problem, 50 years on. Science 2012;338:1042–6. http://dx.doi.org/10.1126/science.1219021.
[7] Salsbury Jr FR. Molecular dynamics simulations of protein dynamics and their relevance to drug discovery. Curr Opin Pharmacol 2010;10:738–44. http://dx.doi.org/10.1016/j.coph.2010.09.016.
[8] Vogiatzis KD, Polynski MV, Kirkl JK, Townsend J, Hashemi A, Liu C, et al. Computational approach to molecular catalysis by 3d transition metals: Challenges and opportunities. Chem Rev 2019;119:2453–523. http://dx.doi.org/10.1021/acs.chemrev.8b00361.
[9] Jacobson LD, Bochevarov AD, Watson MA, Hughes TF, Rinaldo D, Ehrlich S, et al. Automated transition state search and its application to diverse types of organic reactions. J Chem Theory Comput 2017;13:5780–97. http://dx.doi.org/10.1021/acs.jctc.7b00764.

[10] Prampolini G, Campetella M, Mitri NDe, Livotto PR, Cacelli I. Systematic and automated development of quantum mechanically derived force fields: The challenging case of halogenated hydrocarbons. J Chem Theory Comput 2016;12:5525–40. http://dx.doi.org/10.1021/acs.jctc.6b00705.
[11] Bannwarth C, Ehlert S, Grimme S. GFN2-xTB—An accurate and broadly parametrized self-consistent tight-binding quantum chemical method with multipole electrostatics and density-dependent dispersion contributions. J Chem Theory Comput 2019;15:1652–71. http://dx.doi.org/10.1021/acs.jctc.8b01176.
[12] Grimme S. Exploration of chemical compound conformer, and reaction space with meta-dynamics simulations based on tight-binding quantum chemical calculations. J Chem Theory Comput 2019;15:2847–62. http://dx.doi.org/10.1021/acs.jctc.9b00143.
[13] Grimme S, Bannwarth C, Dohm S, Hansen A, Pisarek J, Pracht P, et al. Fully automated quantum-chemistry-based computation of spin–spin-coupled nuclear magnetic resonance spectra. Angew Chem Int Ed 2017;56:14763–9. http://dx.doi.org/10.1002/anie.201708266.
[14] Grimme S, Bohle F, Hansen A, Pracht P, Spicher S, Stahn M. Efficient quantum chemical calculation of structure ensembles and free energies for nonrigid molecules. J Phys Chem A 2021;125:4039–54. http://dx.doi.org/10.1021/acs.jpca.1c00971.
[15] Guan Y, Ingman VM, Rooks BJ, Wheeler SE. AARON: An automated reaction optimizer for new catalysts. J Chem Theory Comput 2018;14:5249–61. http://dx.doi.org/10.1021/acs.jctc.8b00578.
[16] Valiev M, Bylaska EJ, Govind N, Kowalski K, Straatsma TP, Van Dam HJJ, et al. NWChem: A comprehensive and scalable open-source solution for large scale molecular simulations. Comput Phys Comm 2010;181:1477–89. http://dx.doi.org/10.1016/j.cpc.2010.04.018.
[17] Lin S, Fromer JC, Ghosh Y, Hanna B, Elanany M, Xu W. Computer-assisted catalyst development via automated modelling of conformationally complex molecules: application to diphosphinoamine ligands. Sci Rep 2021;11:4534. http://dx.doi.org/10.1038/s41598-021-82816-x.
[18] Barman S, Jaseer EA, Garcia N, Elanany M, Khawaji M, Xu W, et al. A rational approach towards selective ethylene oligomerization via PNP-ligand design with an N-triptycene functionality. Chem Commun 2022;58:10044–7. http://dx.doi.org/10.1039/D2CC02456J.
[19] Luchini G, Alegre-Requena J, Funes-Ardoiz I, Paton R. GoodVibes: automated thermochemistry for heterogeneous computational chemistry data. F1000Research 2020;9:291. http://dx.doi.org/10.12688/f1000research.22758.1.
[20] Dohm S, Bursch M, Hansen A, Grimme S. Semiautomated transition state localization for organometallic complexes with semiempirical quantum chemical methods. J Chem Theory Comput 2020;16:2002–12. http://dx.doi.org/10.1021/acs.jctc.9b01266.
[21] Grimme S. Supramolecular binding thermodynamics by dispersion-corrected density functional theory. Chem Eur J 2012;18:9955–64. http://dx.doi.org/10.1002/chem.201200497.
[22] Grimme S, Antony J, Ehrlich S, Krieg H. A consistent and accurate ab initio parametrization of density functional dispersion correction (DFT-D) for the 94 elements H-Pu. J Chem Phys 2010;132:154104. http://dx.doi.org/10.1063/1.3382344.
[23] Andrea NB, Steven W. Popular integration grids can result in large errors in DFT-computed free energies. 2019, http://dx.doi.org/10.26434/chemrxiv.8864204.v5, ChemRxiv Preprint.
[24] Wheeler SE, Houk KN. Integration grid errors for meta-GGA-predicted reaction energies: Origin of grid errors for the M06 suite of functionals. J Chem Theory Comput 2010;6:395–404. http://dx.doi.org/10.1021/ct900639.
[25] Weigend F, Ahlrichs R. Balanced basis sets of split valence triple zeta valence and quadruple zeta valence quality for H to Rn: design and assessment of accuracy. Phys Chem Chem Phys 2005;7:3297–305. http://dx.doi.org/10.1039/B508541A.
[26] Weigend F. Accurate Coulomb-fitting basis sets for H to Rn. Phys Chem Chem Phys 2006;8:1057–65. http://dx.doi.org/10.1039/B515623H.
[27] Liu L, Liu Z, Cheng R, He X, Liu B. Unraveling the effects of H2, N substituents and secondary ligands on Cr/PNP-catalyzed ethylene selective oligomerization. Organometallics 2018;37:3893–900. http://dx.doi.org/10.1021/acs.organomet.8b00578.
[28] Hirscher NA, Perez Sierra D, Agapie T. Robust chromium precursors for catalysis: Isolation and structure of a single-component ethylene tetramerization precatalyst. J Am Chem Soc 2019;141:6022–9. http://dx.doi.org/10.1021/jacs.9b01387.
[29] Chapman AM, Haddow MF, Wass DF. Frustrated lewis pairs beyond the main group: Synthesis reactivity, and small molecule activation with cationic zirconocene–phosphinoaryloxide complexes. J Am Chem Soc 2011;133:18463–78. http://dx.doi.org/10.1021/ja207936p.
[30] Wu F, Dash AK, Jordan RF. Structures and reactivity of Zr(IV) chlorobenzene complexes. J Am Chem Soc 2004;126:15360–1. http://dx.doi.org/10.1021/ja044303v.
[31] McGlinchey MJ, Tan T-S. Synthesis and 19F nuclear magnetic resonance spectra of fluorosubstituted bis(arene)chromium complexes. Can J Chem 1974;52:2439–43. http://dx.doi.org/10.1139/v74-355.
[32] Kundig EP, Pache SH. Product class 4: Arene organometallic complexes of chromium, molybdenum, and tungsten. In: Imamoto T, editor. Category 1, Organometallics, Volume 2. Stuttgart: Georg Thieme Verlag KG; 2003, http://dx.doi.org/10.1055/sos-SD-002-00214.
[33] Starovskii OV, Struchkov YT. Crystal structure of ditoluenechromium iodide. J Struct Chem 1961;2:152–61. http://dx.doi.org/10.1007/BF00750992.
[34] Lifschitz AM, Hirscher NA, Lee HB, Buss JA, Agapie T. Ethylene tetramerization catalysis: Effects of aluminum-induced isomerization of PNP to PPN ligands. Organometallics 2017;36:1640–8. http://dx.doi.org/10.1021/acs.organomet.7b00189.
[35] Bergwerf H. MolView. 2020, Accessed19May2020.
[36] Halgren TA. Merck molecular force field. I. Basis, form, scope, parameterization, and performance of MMFF94. J Comput Chem 1996;17:490–519. http://dx.doi.org/10.1002/(sici)1096-987x(199604)17:5/6<490::Aid-jcc1>3.0.Co;2-p.
[37] McGuinness DS, Chan B, Britovsek GJP, Yates BF. Ethylene trimerisation with Cr-PNP catalysts: A theoretical benchmarking study and assessment of catalyst oxidation state. Aust J Chem 2014;67:1481–90. http://dx.doi.org/10.1071/CH14436.
[38] Britovsek GJP, McGuinness DS. A DFT mechanistic study on ethylene Tri- and tetramerization with Cr/PNP catalysts: Single versus double insertion pathways. Chem Eur J 2016;22:16891–6. http://dx.doi.org/10.1002/chem.201603909.
[39] Fan H, Alam F, Hao B, Ma J, Zhang J, Ma Z, et al. Rationalizing the catalytic performance of Cr(III) complexes stabilized with alkylphosphanyl PNP ligands for selective ethylene tri-/tetramerization: a DFT study. Theor Chem Acc 2022;141:25. http://dx.doi.org/10.1007/s00214-022-02887-5.
[40] Kwon D-H, Fuller JT, Kilgore UJ, Sydora OL, Bischof SM, Ess DH. Computational transition-state design provides experimentally verified Cr(PN) catalysts for control of ethylene trimerization and tetramerization. ACS Catal 2018;8:1138–42. http://dx.doi.org/10.1021/acscatal.7b04026.
[41] Liu L, Liu Z, Tang S, Cheng R, He X, Liu B. What triggered the switching from ethylene-selective trimerization into tetramerization over the Cr/(22′-dipicolylamine) catalysts? ACS Catal 2019;9:10519–27. http://dx.doi.org/10.1021/acscatal.9b03340.
[42] Rackers JA, Wang Z, Lu C, Laury ML, Lagardère L, Schnieders MJ, et al. Tinker 8: Software tools for molecular design. J Chem Theory Comput 2018;14:5273–89. http://dx.doi.org/10.1021/acs.jctc.8b00529.
[43] Schlegel HB. Geometry optimization. WIREs Comput Mol Sci 2011;1:790–809. http://dx.doi.org/10.1002/wcms.34.
[44] Schlegel HB. Exploring potential energy surfaces for chemical reactions: An overview of some practical methods. J Comput Chem 2003;24:1514–27. http://dx.doi.org/10.1002/jcc.10231.
[45] Zimmerman PM. Single-ended transition state finding with the growing string method. J Comput Chem 2015;36:601–11. http://dx.doi.org/10.1002/jcc.23833.